



This is a repository copy of *A CFD analysis of several design parameters of a road pavement solar collector (RPSC) for urban application.*

White Rose Research Online URL for this paper:
<http://eprints.whiterose.ac.uk/112558/>

Version: Accepted Version

Article:

Nasir, D.S.N.M., Hughes, B.R. and Calautit, J.K. (2016) A CFD analysis of several design parameters of a road pavement solar collector (RPSC) for urban application. *Applied Energy*, 186 (3). pp. 436-449. ISSN 0306-2619

<https://doi.org/10.1016/j.apenergy.2016.04.002>

Reuse

This article is distributed under the terms of the Creative Commons Attribution-NonCommercial-NoDerivs (CC BY-NC-ND) licence. This licence only allows you to download this work and share it with others as long as you credit the authors, but you can't change the article in any way or use it commercially. More information and the full terms of the licence here: <https://creativecommons.org/licenses/>

Takedown

If you consider content in White Rose Research Online to be in breach of UK law, please notify us by emailing eprints@whiterose.ac.uk including the URL of the record and the reason for the withdrawal request.



eprints@whiterose.ac.uk
<https://eprints.whiterose.ac.uk/>

1 **A CFD Analysis of Several Design Parameters of**
2 **A Road Pavement Solar Collector (RPSC) for Urban Application**

3 **Diana SNM Nasir ^{a*}, Ben Richard Hughes ^a, John Kaiser Calautit ^a**

4
5 ^a Energy 2050, Department of Mechanical Engineering, The University of Sheffield, Sheffield, S1 3JD, United Kingdom

6 * Corresponding author. Email: sdnbintimohdnasir1@sheffield.ac.uk; Tel. +44(7) 424 289 937

7
8 **Abstract**

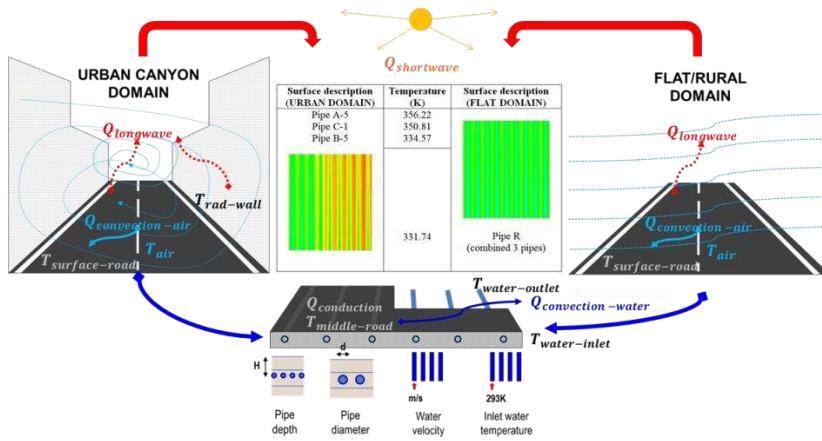
9 Previous investigations of the Urban Heat Island (UHI) effects have highlighted the long-term
10 negative impacts of urban street canyons on surroundings temperatures that indirectly contribute to
11 global warming. Studies on road pavement solar collector (RPSC) system have shown the potential of
12 reducing the heat from the pavement surface by absorbing the heat from the pavement and harnessing
13 the thermal energy. This study expands the investigation of optimising the RPSC system based on
14 four tested parameters (pipe diameter, pipe depth, water velocity and water temperature) comparing
15 the system performance in terms of Delta T of inlet-outlet, potential thermal collection (PTC) and
16 surface temperature reduction (STR). Two types of external environmental conditions were
17 considered: (i) urban domain resembling a street canyon (ii) flat surface resembling a low density or
18 rural area. ‘De-coupled’ CFD method was employed based on previously author’s published work by
19 simulating the effect of external environment (macro domain) onto RPSC system (micro domain) in
20 two separate CFD modelling. Initially, both domains were validated with numerical and experimental
21 data from previously published works. In comparing the RPSC application in urban domain and
22 flat/rural domain; it was found that the system adjustment based on high and low conditions of water
23 velocity provided the best performance improvement with average 28 % higher in terms of PTC and
24 STR as compared to other simulated parameters. Yet, insignificant Delta T (less than 5 K) was
25 obtained with values over 0.02 m in the pipe diameter and in the 0.25 m/s water velocity.

26
27 **Keywords:** Road solar collector, hydroponic pipes, urban canyon, computational fluid dynamic
28 (CFD), urban heat island (UHI)

29
30 **Number of words: 7553**

1 **Graphical Abstract**

2



3

4

5 **Nomenclature**

6

Term	Description
T_a	Air temperature, K
$T_{1,s}$	Ground surface temperature, K
$T_{w,i}$	Area-weighted average inlet water temperature, K
$T_{w,o}$	Area-weighted average outlet water temperature, K
c_a	Concentrated canyon area
ASC	Asphalt solar collector
Delta T	Variance in average water outlet temperature and average water inlet temperature, K
DO	Discrete Ordinate radiation model
H	Building height, m
PTC	Potential thermal collection, %
RPSC	Road pavement solar collector
STR	Surface temperature reduction, %
T	Simulated temperature at z-direction, K
UHI	Urban Heat Island
UTC	Universal Time Coordinated
W	Building width, m
$k - \epsilon$	K-epsilon turbulence model

7

8

9

1 **1 Introduction**

2 Recently, works have been focussed on evaluating the system performance of road pavement solar
3 collector (RPSC) in mitigating the Urban Heat Island (UHI)¹ effect during summertime or hot
4 conditions and to speed up the snow melting effect during wintertime. In general, the system works by
5 allowing heat to be transferred from a hotter medium to colder medium. Despite its potential to be an
6 alternative urban energy generator, it should be noted that the initial reason of conceptualising RPSC
7 is to deal with high temperature gradients within road layers caused by the exposed pavement to the
8 excessive solar radiation especially during long day hours. Such high temperature gradient is
9 associated with long-term structural damage and curling problem thus several important studies have
10 conducted thermophysical analysis on tested road materials. Asphalt material which is conventionally
11 used for road construction was observed to obtain the highest temperature in the afternoon and in the
12 evening as compared to the other studied materials [1]. It has been suggested by [2] that the
13 incapability of the material to dissipate heat fully before sunrise can cause the occurrence of heat
14 effect in the early morning. The temperature gradient of concrete slab was calculated as high as 18°C
15 when the lowest and the highest slab temperature values were compared. The work suggested that
16 more investigations are necessary to improve the current state of road materials in order to prolong the
17 lifespan.

19 **2 Literature review**

20 According to [3], reduction in the surface temperature of 5°C was emphasised to extend the lifecycle
21 of the pavement up to 5 years [4] meanwhile in the study of [5], the reduction between 3°C and 4°C in
22 the surface temperature or 6°C in the total daily cycle fluctuation has been predicted to significantly
23 delay the pavement cracking and structural damage during the exposed daytime. In the early 90s,
24 alternative pavements with the increased values in the solar reflectance, thermal emittance and
25 convection coefficient for surface temperature reduction were discussed to replace the conventional
26 asphalt pavement [6]. It was highlighted in the study of [7] that during the exposed time to sunlight;
27 the conductive asphalt was observed has speed up the heat conduction in the top-down direction
28 across the specimen layers, reducing the potential to increase the temperature gap between the
29 specimen depths. Recently, studies have found the connectivity of the exposed urban surfaces to
30 influence in three aspects to determine the condition of an urban area: (i) climate, (ii) thermal comfort,
31 and (iii) electricity usage. In the study of [8], it was reported that the increase between 2% to 4% in
32 the electric demand was due to 1°C rise in the daily maximum air temperature with the range of 15-
33 20°C. The problem was associated with the exposed dark asphalt surface to the solar radiation which
34 tends to absorb more heat than other type of urban surfaces. This study found the importance of using

¹ According to Elsayed (2006) [44], UHI effect is the rise in urban air temperature as compared to rural areas caused by urban elements, urban land use pattern, artificial heat production, displacement of natural elements, urban pollution and human activities.

1 high reflective pavement(s) to reduce the absorptivity factor while increasing the emissivity value of
2 the pavement surface(s); to be called ‘cool pavements’. Analysis by using numerical simulation has
3 found a significant 10°C temperature reduction from the urban road surface by the increase of 0.25 in
4 the surface albedo. Consequently, cool pavement analysis was carried out to evaluate the influence on
5 the external environment of Los Angeles within one-third of the city area by using a similar method
6 [9]. This has brought the prediction that by reducing 1.5°C in the air temperature, the city can save
7 approximately 100 megawatts per hour in the demand for electricity. Thus, [8] suggested the
8 importance of using light coloured asphalt or light asphalt mixtures; however it should also be noted
9 that in the study of [10] seems not fully agreed. While numerous studies have found the potential of
10 modifying the surface albedo for UHI mitigation; the study of [10] found that high reflective material
11 can reduce the level of external thermal comfort of the nearby pedestrian by integrating models
12 developed by [11, 12].

13

14 **2.1 RPSC system integration to conventional pavement**

15 As early as 1988, the use of underground pipe was mentioned to have the potential for fuel saving
16 apart from road heating during winter season [13]. Additionally, the use of hydronic pipes for
17 cooling/heating has been well documented under ASHRAE standard [14]. In hot climate condition,
18 studies have correlated the use of hydronic pipes to reduce the surface temperature of road pavements.
19 It was highlighted in the study of [15] that the hydronic RPSC was observed to perform well in
20 cooling the pavement and for thermal storing when the coolant temperature was within the range of
21 18°C-24°C. In the study of [16], field test measurement was carried out to integrate hydronic RPSC
22 tubes within 135mm depth from the asphalt surface. An experimental study in Tokyo during summer
23 season has introduced the utilisation of nearby resources (river water) to support the pavement-pipe
24 heat transfer process which is called ‘Road Thermal Energy Conversion’ (RTEC) system [17]. The
25 system was designed by connecting a thermoelectric generator with 10 mm diameter heat exchanger
26 pipes and to be embedded 70 mm underneath a road surface, reducing the surface temperature by 9 %
27 on average as compared to the conventional pavement without RTEC.

28

29 A review of RPSC was carried out by [18] which discussed the system development based on the
30 design in the variables and parameters. A laboratory scale study of asphalt pavement integrated with
31 hydronic copper pipe system was carried out to evaluate the thermal response of the integrated system
32 by changing several tested parameters [19]. Significant reduction in the temperature was observed
33 across the pavement layers with additional hydronic circulation as compared to the conventional
34 pavement. Although it was mentioned that the efficiency of the hydronic pipes can be enlarged by
35 increasing the flow rate of the water [20]; it was highlighted in [19] that large increase in the water
36 flow rate did not significantly improve the cooling of the pavement layer. In the similar study has also
37 found that the temperature of the pavement upper layer was reduced by 30 % when the pipe depth was

1 changed from 125 mm to 25 mm. According to a study carried out in United States, it was found that
2 the optimum depth of pipe embedment was 20 mm [18]. In the study of [20], changing the
3 temperature of the inlet water was found to be more appropriate for high speed heat transfer. Using
4 high conductive asphalt materials such as graphite powder, steel fibres, etc were tested by [21, 22, 23]
5 to optimise the performance of hydronic pipes. Despite of the experiment was setup for heavy snow
6 condition [21], it should be noted that a 50% increase in the thermal conductivity of the asphalt
7 pavement has increased about 30% of the system performance.

8
9 Several works have integrated different types of hybrid RPSC system. For example in the study of
10 [24]; hydronic RPSC which was designed for bridge deck was connected to a Ground-Source Heat
11 Pump (GSHP). The combination was to prevent heavy snow effect on road whereas during
12 summertime, the absorbed heat from RPSC will be streamed down to GSHP as the main heat storage
13 system in long-term basis. Another example can also be found in [15]. In the study of [25], ‘GSHP
14 combined Ground Heat Exchanger (GHE)’ was designed in the U-shape 40 mm diameter heat
15 exchanger tubes and were inserted in the drilled vertical borehole with three depth values (30 m, 60 m
16 and 90 m) for comparative analysis. The study highlighted that the longest drilled borehole has the
17 highest coefficient of performance by 50% over the shortest drilled borehole. For the similar
18 combination, temperature distribution was then studied; see [26]. Recently, another type of hybrid
19 RPSC was studied which combines thermal energy storage, heat pump, solar panels and wind energy;
20 to be called as ‘Hybrid Renewable Heating System’ (HRES) [27].

21 22 **2.2 Integrated system with urban environment**

23 This paper has broadened another perspective of evaluating RPSC system for urban application which
24 has to deal with the urban climate and its complexity to comprehend heat effect on urban surfaces. It
25 was mentioned earlier regarding the obtained high pavement temperature which can affect the
26 climate, comfort and electricity usage of the surroundings. Conversely, it should also be highlighted
27 that the city land surface is not as simple as a flat surface. In the study of [8, 28], urban geometry is in
28 the complex shape and has the influence on the solar heat flux either in short wave or long wave
29 direction, causing heat to be accumulated and increases the temperature of the surroundings.
30 Investigation on the effect of buildings to the air temperature was carried out in the study of [28, 29];
31 also called ‘canyon’ street effect. According to the study [28, 29], it was observed that the long wave
32 reflection from ground to sky can be decelerated due to the increase in the aspect ratio of the canyon².
33 A good comparative 2-dimensional numerical model was developed in 2012 [30] to analyse the effect
34 on air temperature within the scenario of having building canyon and without (flat surface). In recent
35 years, many works have extensively used computational methods to carry out evaluations of the

² As referred to the study of Levermore and Cheung (2012); street canyon aspect ratio, H/W is a ratio of building height, H to the width of a street canyon, W [30]

1 microclimate and thermal issues on urban environment. Computational Fluid Dynamic (CFD)
2 analysis has the ability to solve problem related to fluid flow from a simplified geometry model [31]
3 to the complicated one [32].
4

5 **2.3 Aim and objective**

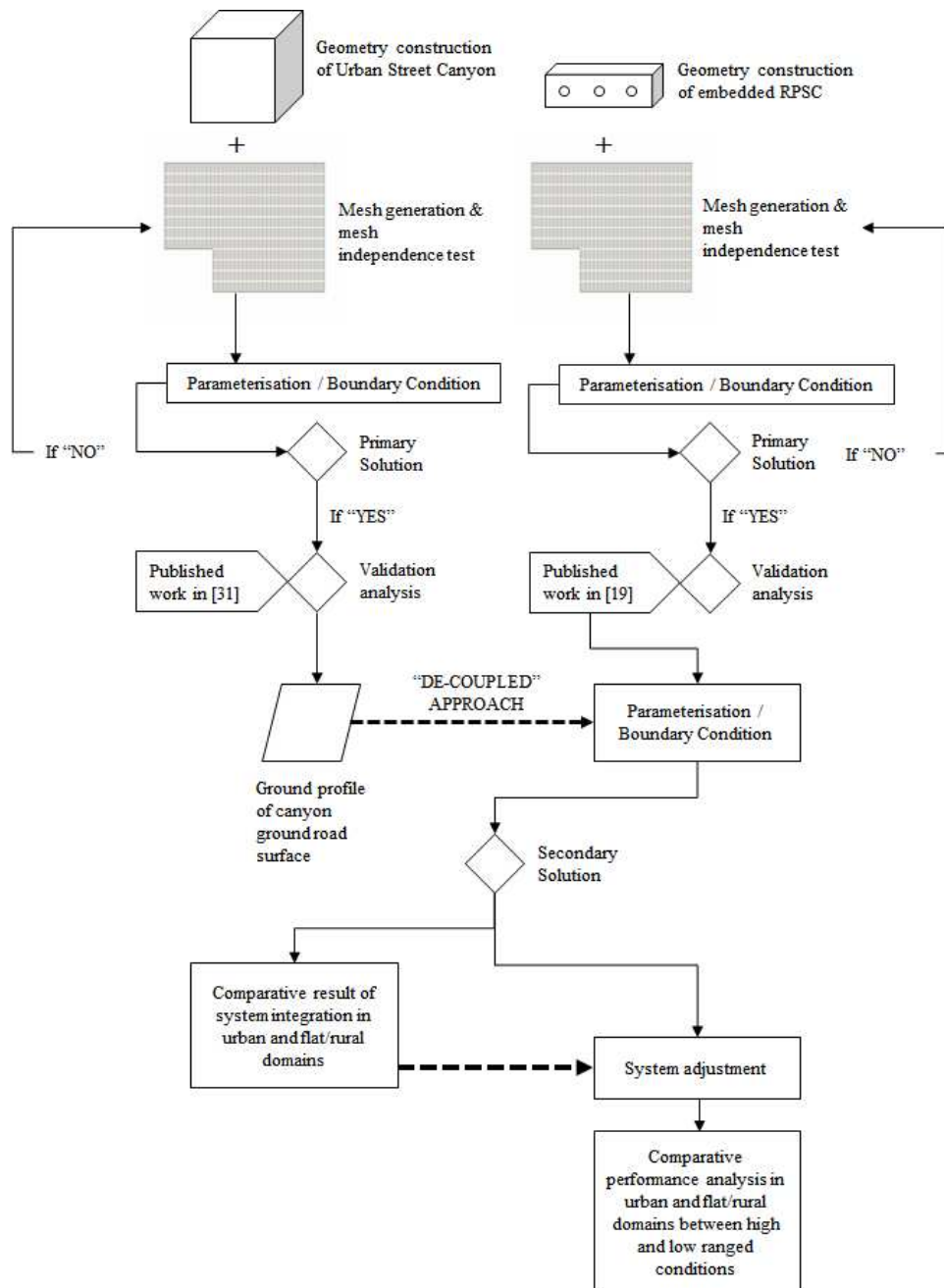
6 To the authors' knowledge and after conducting a comprehensive study, there is no work on the
7 analysis of the design parameters of RPSC system which includes the impact of urban environment.
8 Therefore; to address the current gap in the literature, this paper evaluates the performance of RPSC
9 when the surface of the system embedment is located in between two buildings replicating an urban
10 scenario. Several studies have noted the significant impact of wind on the heat loss from the pavement
11 surface [26, 33] meanwhile in the study of [31, 34], wind-blocking building orientation was found to
12 cause deceleration of wind velocity on the ground surface which also reduced the convective heat
13 transfer from the surface. Another important effect of buildings on ground surface is the shadow;
14 which can cause less heat flux received by the surface [35]. Thus, thermal performance of RPSC
15 within two dissimilar conditions of embedment will be compared: (i) surface with building rows –
16 canyon/urban environment, and (ii) surface without building rows – flat surface/rural environment. A
17 'de-coupled' computational modelling has been employed following the method detailed in the
18 previous published work [36]. Computational analysis has been carried out in a number of RPSC
19 studies; for example by using Finite Element Model (FEM) [3, 2] and Finite Difference Model (FDM)
20 [5]. The 'de-coupled' approach has combined the 3-dimensional Finite Volume Model (FVM) macro
21 domain which represents the external environment above a pavement surface with a 3-dimensional
22 FVM micro domain which represents the hydronic RPSC system. To evaluate the performance of
23 RPSC system within an urban environment and also flat/rural environment, this study assesses the
24 effect of changing several system parameters such as: (i) pipe diameter, (ii) water velocity, (iii) pipe
25 depth, and (iv) inlet water temperature. The system parameters have been set within the range as
26 referred to the values of the previous published works with the goal to determine the optimum
27 parameter for urban integration of the RPSC system.
28
29
30
31
32
33
34
35
36
37

1 **3 Methodology: 3-dimensional Finite Volume Method (FVM)**

2

3 **3.1 De-coupled computational modelling**

4 A de-coupled computational modelling method was used to: (i) analyse the effect of building rows or
 5 canyon on the thermal performance of RPSC system, (ii) compare the thermal performance of urban
 6 RPSC with flat/rural RPSC, and (iii) evaluate the optimum values of urban RPSC with system
 7 variables over the flat/rural RPSC; see Figure 1 which details the methodology flow chart.
 8



9 Figure 1: Methodological chart of de-coupled CFD simulation approach

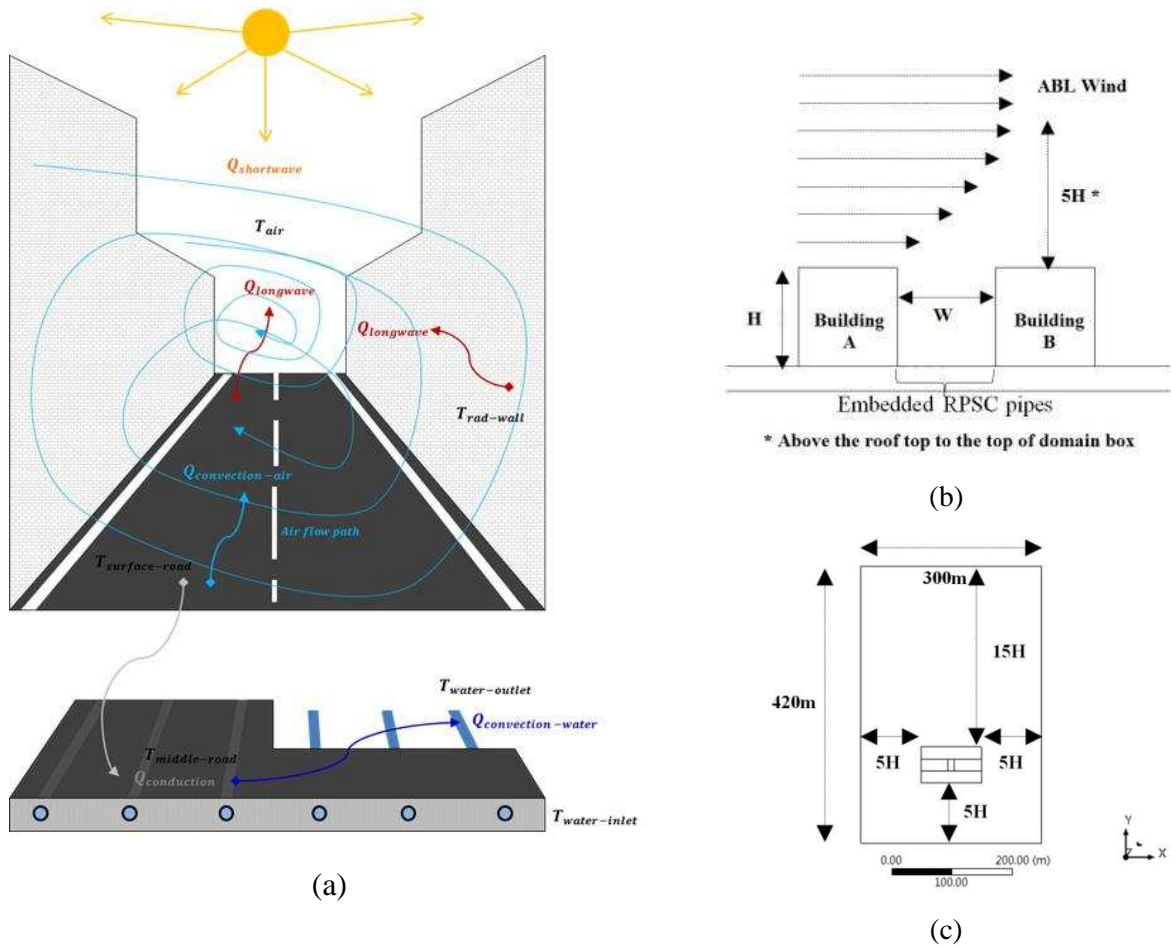
3.2 Computational geometry and domain

A benchmark model was selected based on the previous studies [31, 36] and its criteria were followed to represent an urban street canyon model within a computational flow domain. Two domains were classified as the macro domain which represents the external environment above a pavement surface and the micro domain which represents the RPSC pipe embedded underneath a pavement. For the macro domain, the temperature of a road surface was assumed to be influenced by five variables: (i) solar radiation, (ii) air flow, (iii) canyon geometry, (iv) building wall temperature, and (v) soil temperature. After the model was validated, the temperature output of the surface was obtained and was used as the input for the micro domain model to calculate the heat output from the RPSC system.

3.2.1 Urban macro domain (RPSC-1)

A street canyon model consists of a 20.0 m width road in between two buildings where each building has the dimension of 100.0 m length, (L) 20.0 m width (W) and 20.0 m height (H); to be specified as the canyon aspect ratio (H/W) of 1. The integration of macro-micro domains were visualised as per Figure 2(a) and specification of the urban macro domain was detailed with dimensions in Figure 2(b) and 2(c) [31].

Based on [31, 36], a standard canyon configuration was set up which requires three times larger outflow (15H) than inflow distance (5H) to allow the flow to re-develop behind the recirculation region. Similar distance was set up for the distance to the left and the right domain walls from the side walls of the buildings. For sufficient height for the air flow over between the roof top and the domain top plane, similar distance of 5H was also applied. This macro model was divided in three volumes: (i) air-fluid region (wind flow), (ii) 5.0 m depth solid region (road and soil) and (iii) empty region (building interiors; excluded in the study). The wind inlet plane was oriented parallel to y -direction with the first building wall closer to the inlet plane acting as an obstacle to the incoming wind. This study only considered one street canyon shape with one building orientation.



1 Figure 2: Urban domain (a) in 3-dimensional diagram (b) from elevation view (c) from top view

2

3 3.2.2 Flat/rural macro domain (RPSC-0)

4 Similar guidelines were also applied for an empty macro domain which represents a less dense urban
 5 area or rural area. Two regions were divided in this domain: (i) air-fluid region (wind flow), and (ii)
 6 5.0 m depth solid region (road and soil). Similar location and distances of direction x , y and z were
 7 indicated for the canyon ground road surface. The only difference is the ground road surface was not
 8 sandwiched between two buildings. The overall size of both macro domains was 460.0 m length \times
 9 300.0 m width \times 125.0 m height (5m depth below ground surface).

10

11 3.2.3 RPSC micro domain

12 The RPSC system was characterised by circular hollow horizontal copper pipes with 10 m length,
 13 0.005 m (5 mm) wall thickness and 0.02 m (20 mm) nominal diameter following the study of [37] to
 14 be embedded 0.15 m (150 mm) below the road surface. The gap between the pipes was assumed 1.0
 15 m and the pipes were layered to be parallel with the road direction (north to south). Simplification of
 16 the model was carried out by placing the RPSC pipes at the central area; approximately 10% area was
 17 covered out of the total road surface area. The total area of the pipe embedment was 10.0 m length \times

20.0 m width. For the micro domain, a 10.0 m length pipe was designed to be embedded within a solid pavement with dimension 10.0 m length \times 1.0 m width \times 0.3 m ground depth.

3.3 Mesh

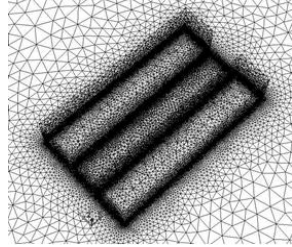
In general, this study applied patch independent hybrid meshing technique on all investigated geometries. The patch independent mesh algorithm is based on the subsequent spatial subdivision algorithm which ensures refinement of the mesh where essential, but retains larger elements where feasible, therefore allowing faster computational times [37].

3.3.1 Macro domains

For the mesh sizing of both macro domains, ‘edge sizing’ was used to refine several canyon sections, c_a which are: (i) canyon ground road surface, (ii) building walls, and (iii) canyon lower ground. ‘Inflation of First Layer Thickness’ option was used to generate very fine mesh near the ground level in order for the mesh to grow gradually in the bottom-up direction. The first layer thickness was set to 0.10 m with growth rate of 1.2; however the maximum layer was set to 20. To determine the optimum size of the mesh, mesh refinement method (h-method) was applied based on the distribution of mesh size, h over a finite element. Furthermore, the edge sizing was set to size the mesh from coarse to fine [38] and the values are described as per Table 1.

Table 1: Mesh setting based on edge sizing

Edge size at c_a (m)	Mesh description	Total element (nos)	Total node (nos)
1.00	Coarse, Hybrid	609,332	213,514
0.50	Medium, Hybrid	1,125,457	373,925
0.25	Fine, Hybrid	2,063,739	659,968



Note: Generated mesh allows finer mesh at the concentrated area

It should be highlighted that similar meshing technique was also applied for the empty domain (no building). Although the buildings are absent from the domain, refinement of the mesh was set near the surface where the embedment of the RPSC pipes was designated. In the previous study [36], the error was very nominal when comparing the coarse, medium and fine meshes (overall less than 0.50 % in difference). This study has carried out the simulation for both macro domains in fine mesh sizing due to very high speed computational time still can be achieved. Table 2 displays the details of the selected sizing for urban and empty domains. It can be observed that 2.67 % was deducted from the total nos of element and node of empty domain.

1 Table 2: Description on the selected mesh sizing for macro domains

Domain	Selected sizing	Total element (nos)	Total node (nos)
Urban/building canyon	Fine, verified	2,063,739	659,968
Flat/no building	Fine, verified	2,010,784	731,198

2

3 3.3.2 Micro domain

4 To determine the meshing type of micro domain, the pipe body was set in the size of 0.020 m (20
5 mm); dividing the total length into 2000 elements with 0.005m sizing each (5 mm). This setting has
6 automatically generated 0.02 m × 0.02 m hexahedral grid for upper and lower layers while the
7 thickness is gradually reduced when the layers are closer to the pipe body.

8

9 **3.4 Boundary conditions**

10

11 3.4.1 Study background

12 The location of the simulated building was in Milan of the north Italy [31, 36, 39] with the longitude
13 of 9.18°E, latitude of 45.47°N and the UTC of +1. It was reported in the study of [39] that the summer
14 days in Milan is the combination of hot temperature with low winds. The selected time, date, month,
15 the intensity of the solar radiation, air velocity, air turbulent intensity, the ambient temperature and the
16 ground roughness condition were set based on previous studies [36]. For both buildings, similar
17 conditions of the surfaces were applied. Detailed description of the surface properties is displayed in
18 Table 3.

19

20 Table 3: Boundary condition applied to wall surfaces [36]

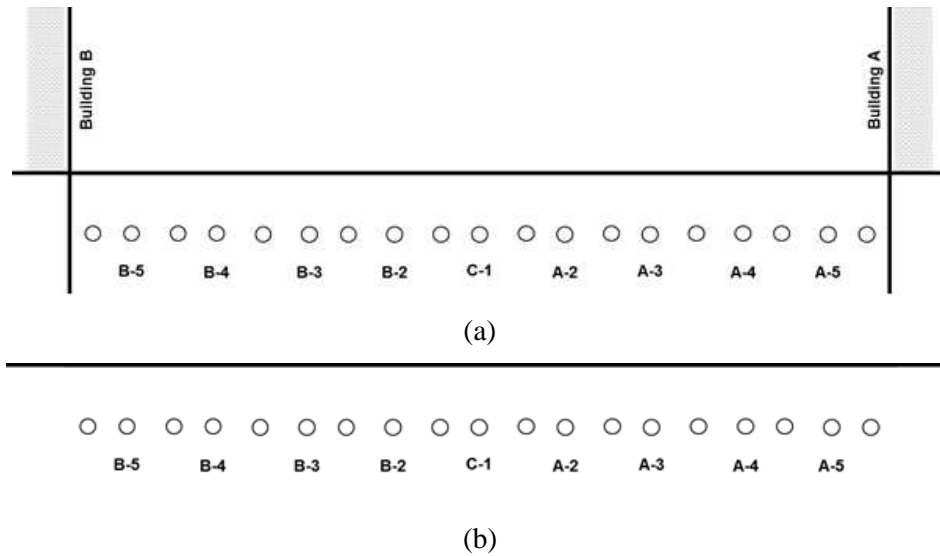
Surface description	Temperature (K)	Density (kg/m3)	Specific heat (J/kgK)	Emissivity	Thermal conductivity (W/mK)
Road surface	Not applied	1000	1000	0.9	2
Soil	288	1000	1000	0.9	2
Building walls	299	1000	1000	0.9	0.15
Copper pipe	Not applied	8978	381	0.8	387.6
Water	293	998.2	4182	Not applied	0.6

21

22 The surface temperatures of the two specified macro domains (urban and flat/rural) were compared
23 and were compared and were exported as the surface condition for the micro domain. It was also
24 highlighted that the analysis of the RPSC performance was carried out for 9 selected pipes based on
25 every two pipes gap (2m distance centre-to-centre). For the urban domain, the selection was carefully
26 measured from the very centre pipe location (pipe C-1) towards building wall A (A-2, A-3, A-4, A-5)

1 and towards building wall B (B-2, B-3, B-4, B-5) as shown in Figure 3(a). Similar selected pipes for
 2 urban domain were also determined for flat/rural domain; see Figure 3(b).

3



4 Figure 3: Embedment of RPSC pipes in (a) urban model (b) flat/rural model (Not to Scale)

5

6 The velocity of the inlet water was set as 0.1 m/s assuming very low speed of water was used [36, 40]
 7 while the inlet water temperature was set 293 K (20°C) which was within the acceptable range [18].
 8 Then, changes involved with four system parameters were evaluated for further comparison between
 9 urban RPSC and flat/rural RPSC as described in 3.4.2, 3.4.3, 3.4.4 and 3.4.5.

10

11 3.4.2 Change in pipe diameter

12 Sizes in RPSC pipe diameter were set from the very small to the very large with the optimum water
 13 velocity according to the diameter: (i) 0.015 m - 0.21 m/s, (ii) 0.02 m - 0.22 m/s, (iii) 0.025 m - 0.32
 14 m/s, (iv) 0.035 m - 0.34 m/s, (v) 0.05 m - , (vi) 0.065 m - , and (vii) 0.075 m - [15, 37, 40]. This
 15 analysis is referred to the rule of thumb by [40] that highlighted that higher pipe diameter requires
 16 higher flow rate to ensure an optimal water flow rate is according to the size of the pipe opening. For
 17 all diameter sizes, the inlet water temperature was set to 293 K (20°C).

18

19 3.4.3 Change in pipe depth

20 Change in the pipe distance from the surface was evaluated by setting up the depth of: (i) 0.025 m, (ii)
 21 0.05 m, (iii) 0.075 m, (iv) 0.1 m, (v) 0.125 m, and (vi) 0.15 m [18, 38, 40, 41]. This simulation
 22 considered one water velocity for every changing depth, 0.1 m/s [40] meanwhile the pipe diameter
 23 was set to 0.02 m with the inlet water temperature of 293 K (20°C).

24

25

1 3.4.4 The effect of water velocity

2 The effects of water velocity for 0.02 m diameter RPSC pipe with 293 k (20°C) water temperature
3 were evaluated from the lowest to the highest settings as per mentioned: (i) 0.1 m/s, (ii) 0.25 m/s, (iii)
4 0.5 m/s, (iv) 0.75 m/s, (v) 1 m/s, (vi) 1.25 m/s, (vii) 1.5 m/s, and (v) 2.0 m/s.

5

6 3.4.5 The effect of water inlet temperature

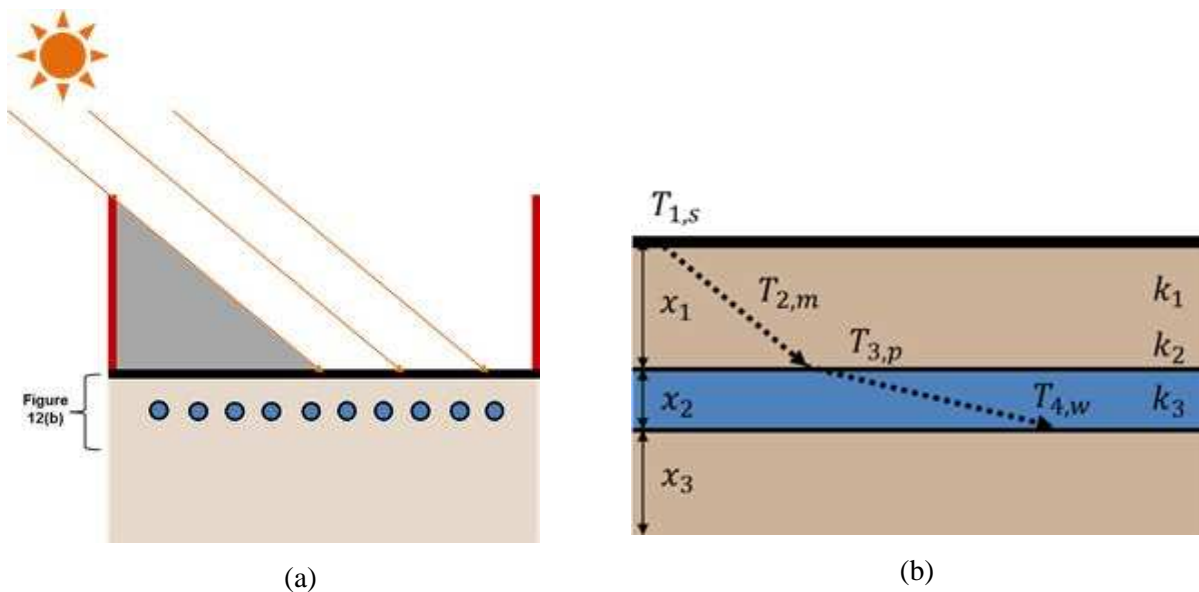
7 Investigation was further carried out to by changing the inlet water temperature. Five inlet water
8 temperatures were analysed: (i) 278K, (ii) 283K, (iii) 288K, (iv) 293K, and (v) 298K [18, 37, 21]. For
9 this analysis, 0.1 m/s water velocity was set with 293 K (20°C) in the inlet water temperature and
10 0.02m in the pipe diameter.

11

12 **3.5 Simulation model**

13 For the radiation model, Discrete Ordinate (DO) was used [37]. Solar Ray Tracing of the Solar Load
14 Model was coupled in order to include the effect of solar radiation in the 3D simulation. To calculate
15 sun radiation, the model requires the global sun location in the sky at a specified date, time zone,
16 longitude-latitude position and sunshine factor [38]. Simulating urban turbulent air flow was based on
17 the principle of momentum, continuity and heat conservation that used steady RANS equations with
18 standard $k-\epsilon$ model. The air flow was assumed to be fully turbulent solved by the transport equation
19 for turbulence kinetic energy (k) and dissipation rate (ϵ) [37]. The simulation involved the conductive
20 and convective heat transfer from the horizontal surface to the bottom layer(s) consisting of pavement
21 solid and the pipe body with flowing medium (water) as demonstrated in Figure 4(a) and 4(b).

22



23 Figure 4: Diagram of heat transfer of (a) external to surface micro domain (b) surface to internal

24

In Figure 4(a), the thermal energy was transferred from the solar radiation to the ground surface and due to the blocking wall from the left side, some parts of the surface area was covered with wall shadow. Figure 4(b) is a blow-up diagram highlighting temperature, T and thermal conductivity, k at different mediums. Each medium represents the material that has different ability to transfer heat from one wall to another.

3.6 Performance calculation

In this study, the calculation of RPSC performance is quantified based on Delta T, Potential Temperature Collection, PTC (%) and Surface Temperature Reduction, STR (%) as per Equation 1, Equation 2 and Equation 3, respectively.

$$\text{Delta T (K)} = T_{w,o} - T_{w,i} \quad (\text{Equation 1})$$

Where Delta T is based on the difference between the inlet water temperature, $T_{w,i}$ (K) and the outlet water temperature, $T_{w,o}$ (K). To calculate PTC, the derived value is obtained by percentage of Delta T per inlet water temperature value, $T_{w,i}$ (see Equation 2). The STR value is the percentage based on the deduction value of the surface temperature, $T_{1,s}$ (K) to the outlet water temperature, $T_{w,o}$ is required per surface temperature, $T_{1,s}$ (see Equation 3).

$$\text{Potential Temperature Collection, PTC (\%)} = \left(\frac{\text{Delta } T}{T_{w,i}} \right) \times 100\% \quad (\text{Equation 2})$$

$$\text{Surface Temperature Reduction, STR (\%)} = \left(\frac{T_{1,s} - T_{w,o}}{T_{1,s}} \right) \times 100\% \quad (\text{Equation 3})$$

In this study, the percentage of the system efficiency was calculated based on the deduction of the value of higher PTC/STR per the lower PTC/STR. For the deficiency, the calculation is as per Equation 5.

$$\text{System efficiency (\%)} \text{ in PTC or STR} = \frac{\text{High value} - \text{Low value}}{\text{Low value}} \times 100\% \quad (\text{Equation 4})$$

$$\text{System deficiency (\%)} \text{ in PTC or STR} = \frac{\text{High value} - \text{Low value}}{\text{High value}} \times 100\% \quad (\text{Equation 5})$$

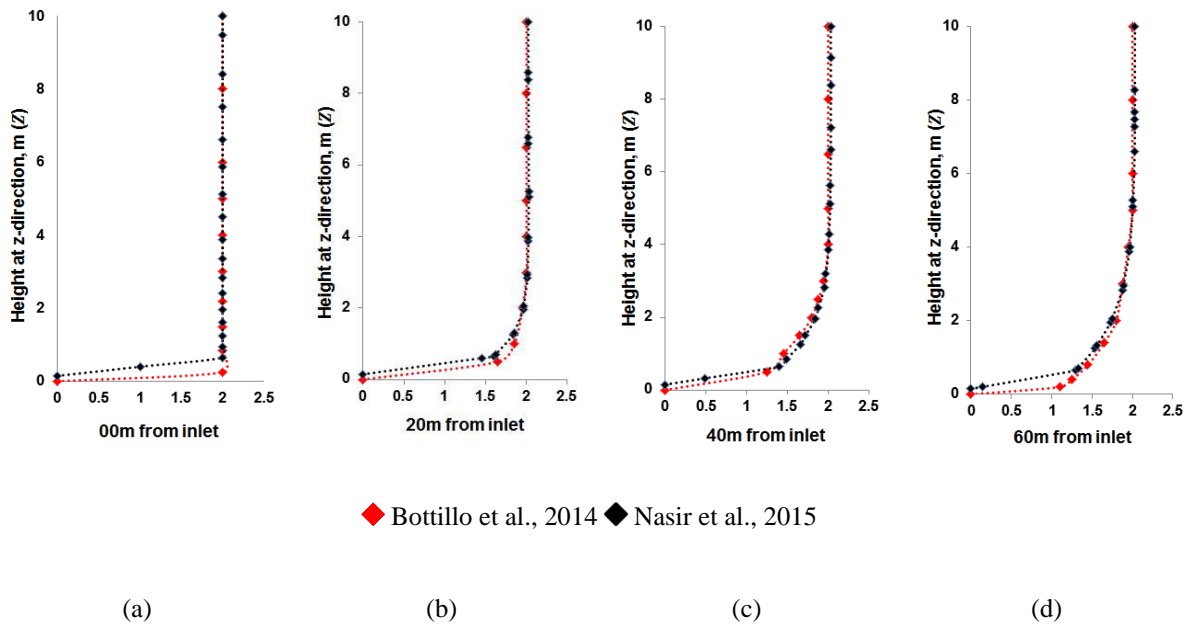
1 **4 Method validation**

2 It was suggested that the simulation works require method validation [5, 17, 21]. However, it should
3 be highlighted that this study has to validate each domain based on an individual analysis due to no
4 integrated study has been carried out before; thus several published works were referred [19, 31, 43].

5
6 **4.1 Macro domain method**

7 For the validation of macro domain, the results were compared against the results of [31, 43] in four
8 analysis: (i) wind profile approaching the first building wall from the inlet plane (Figure 5), (ii)
9 dimensionless air velocity profile in the canyon (Figure 6(a)), (iii) dimensionless air temperature
10 profile in the canyon (Figure 6(b)), and (iv) ground surface temperature measured from selected
11 points (Figure 7).

12



13

14 Figure 5: Validation of wind velocity at four locations based on y-direction

15 (a) 00m from inlet (b) 20m from inlet (c) 40m from inlet (d) 60m from inlet

16

17 Based on Figure 5, the difference between the velocity profile results of the current work and the
18 previous work [31] were less than 1.0 % on average for the plotted profile at 00 m, 20 m, 40 m and 60
19 m from the inlet [36]. In Figure 6(a), it can be observed that the current simulation satisfied the
20 validation of (iii) against wind tunnel experiment of [43] as compared to the previously CFD
21 simulation of [31]; see Figure 6(b).

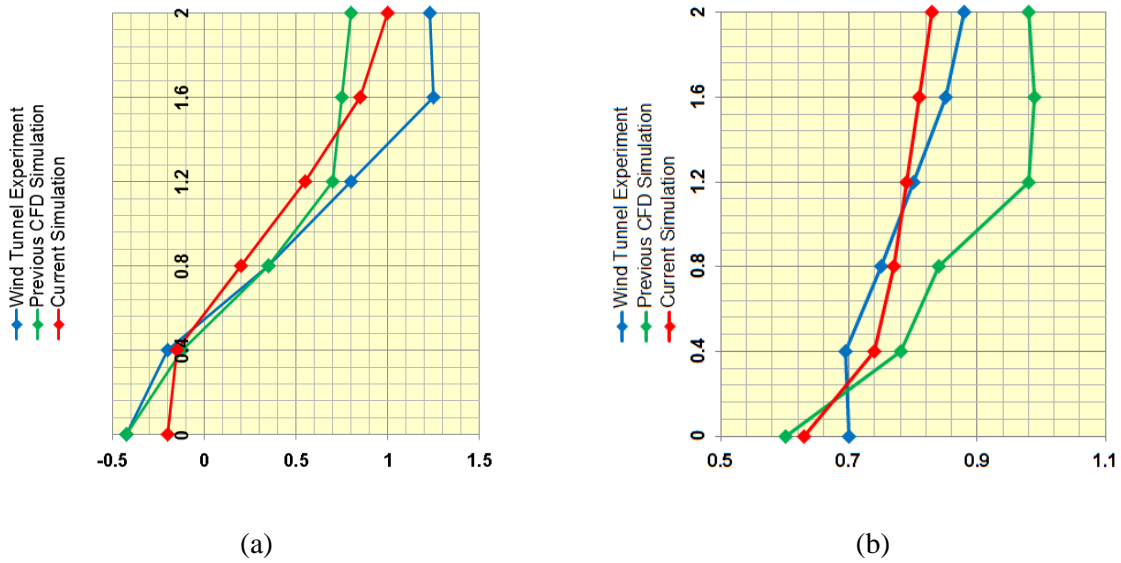


Figure 6: Validation of (a) canyon wind velocity profile (b) canyon air temperature profile

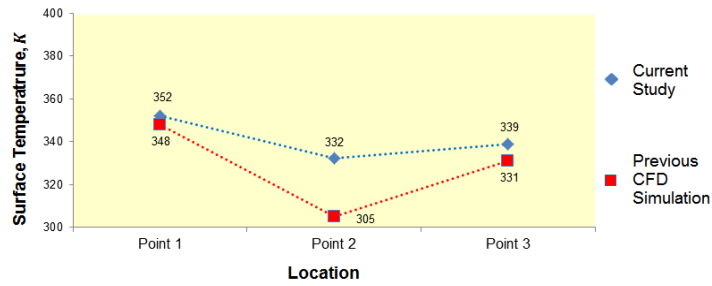


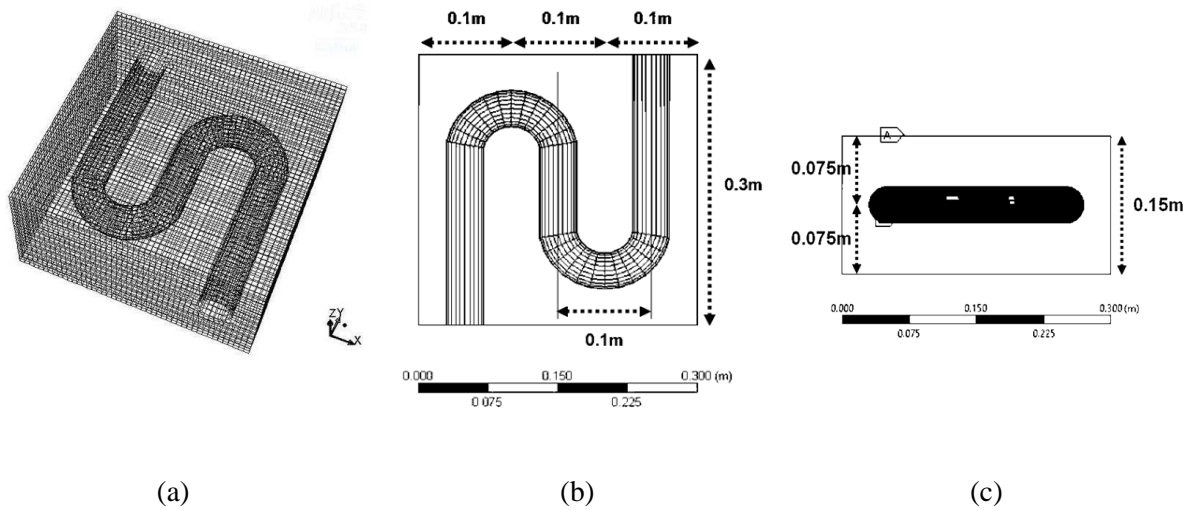
Figure 7: Validation of three temperature points at ground surface

It was found that the error between the current simulation and wind tunnel was 4.57 % on average and the average difference with the previous CFD simulation was 10.61 % on average. For the analysis of (iv), the temperature at Point 1 gave minimal error, 1.15% and for the Point 3, the percentage error was 2.36%; see Figure 7. Point 2 obtained the largest variance with 8.85% difference; however it can be agreed that graph trend was comparable with the reference work. It should be noted that the implemented DO model has dominant values for radiation intensities, causing slightly higher temperature was obtained by the shadowed surface area nearby Building B.

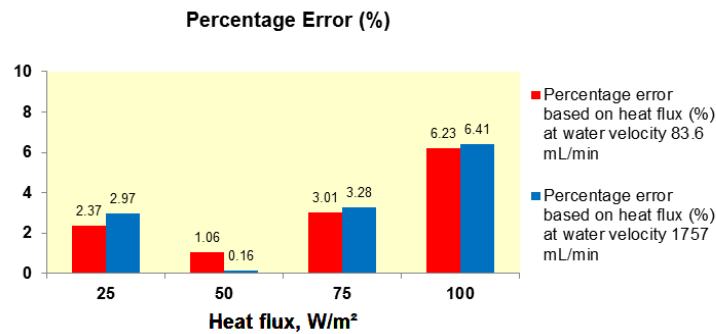
1 **4.2 Micro domain method**

2 The micro domain was validated against the experimental work of [19] which controlled the
 3 surrounding temperature at $25 \pm 1^\circ\text{C}$. The pipe was modelled as per the experimental setup as shown
 4 in Figure 8. To simplify the validation of the model, the surface heat flux of the micro model was set
 5 between 25 W/m^2 and 100 W/m^2 and the selection was based on the lowest percentage error when
 6 compared with the results of the laboratory test; see Figure 9.

7



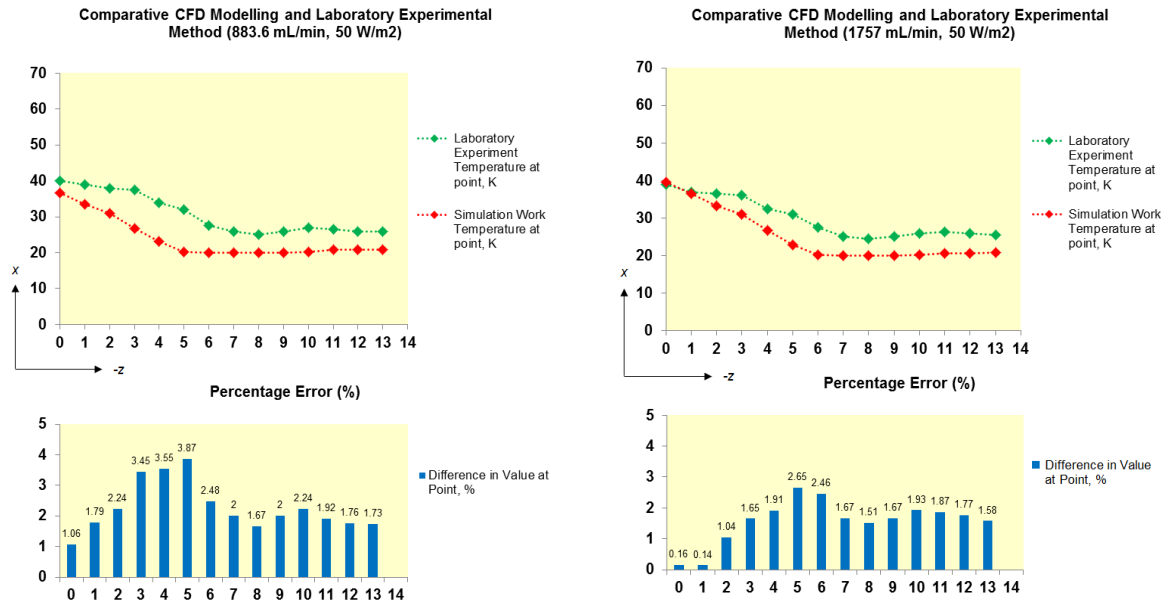
8 Figure 8: Validation configuration of (a) meshing technique (b) plan dimension (c) depth dimension
 9



10 Figure 9: Selection of surface heat flux based on experimental validation error (%)

11

12 Based on Figure 9, 50 W/m^2 surface heat flux provided the lowest percentage error for both water
 13 inlet velocities and was assumed to be the heat flux values in the experiment [19]. To further analyse
 14 and compare the current model with the laboratory work, the temperature distribution within the
 15 pavement depth was plotted (0.0 mm to 140.0 mm) and compared with [19] as displayed in Figure 10.
 16 It was earlier mentioned in Section 2.2 that the two flow rates were tested in [19] to evaluate the effect
 17 on the pavement's temperature distribution.



1 Figure 10: Trend comparison between the current simulation and the experimental results according
 2 to the depth from the surface of (a) 883.6 mL/min (b) 1757 mL/min

3

4 The result demonstrated the heat transfer in top down direction; from the top surface to the bottom
 5 layers of the pavement. Based on the plotted results in Figure 10, it can be noticed that the simulation
 6 of the RPSC has slightly underestimated the experimental results [19].

7

8 4.2.1 Underestimation factor and justification

9 In the laboratory experiment, the surface of the RPSC specimen was exposed to the ambient of the
 10 room, causing the dynamic heat transfer in the bottom-up and the top-down directions while the
 11 circulating water in the pipe was reducing the pavement temperature. It was mentioned earlier that the
 12 surface heat flux has to be assumed 50 W/m²; thus there was no heat exchange occurring between the
 13 pavement surface and the external environment. However, it can be observed that the trend was
 14 similar as compared to the experimental results [19] and the percentage error ranged from 0.14 % to
 15 3.87 %. It was observed that there was no significant difference between the results although there
 16 was large difference in flow rate; which agreed with the observation [19]. Overall, it was observed
 17 that the results of the validation of the simulation method against the published experiment work were
 18 satisfactory and can be used for further analysis.

19

20

21

22

23

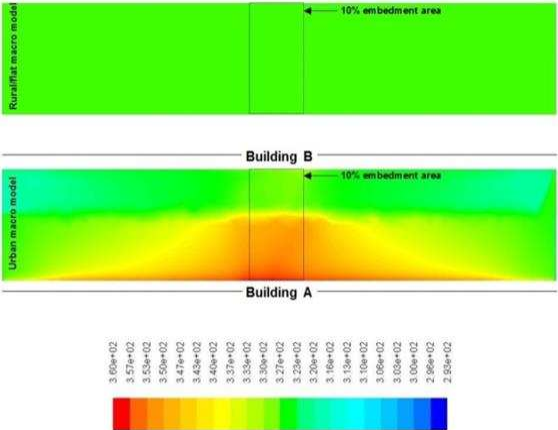
1 **5 Results and discussion**

3 **5.1 Analysis on the surface temperature**

4 Overall, the simulation has demonstrated that the building geometry becomes the major factor to
 5 influence the obtained temperature in the pavement including the surface. This can be clearly
 6 observed in the temperature contours showing lower surface temperature closer to the Building B due
 7 to the shadow effect from the building. Conversely, higher temperature was obtained from the
 8 pavement surface closer to the Building A where the solar radiation was not obstructed by the
 9 building. For the pavement in the flat/rural domain, the simulation showed that the pavement surface
 10 received equal temperature from the solar radiation due to no influence by any building. Table 4
 11 displays the surface temperatures obtained for both macro domains.

13 Table 4: Simulation result of average surface temperature for urban domain and flat/rural domain

Surface description	Temperature (K)
<u>Surfaces of urban domain</u>	
Above 0.15m of pipe A-5.....	356.22
Above 0.15m of pipe A-4.....	353.21
Above 0.15m of pipe A-3.....	352.01
Above 0.15m of pipe A-2.....	351.41
Above 0.15m of pipe C-1.....	350.81
Above 0.15m of pipe B-2.....	342.99
Above 0.15m of pipe B-3.....	334.57
Above 0.15m of pipe B-4.....	334.57
Above 0.15m of pipe B-5.....	334.57
<u>Surfaces of rural domain</u>	
Above 0.15m of all flat/rural pipes (constant surface temperature)	331.74



Note: the temperature measurement was conducted within the 10 % embedment area

14
 15 Average water outlet temperature was calculated by selecting the area weighted average of the pipe
 16 outlet plane and the temperature difference of inlet-outlet selection is represented as Delta T. The
 17 results for Delta T, Potential Thermal Collection (PTC) and Surface Temperature Reduction (STR)
 18 based on the simulation of summer day 21st June at 13:00 hour are summarised in Table 5.

19
 20 Using Delta T, PTC and STR values, the efficiency/deficiency of the system performance in the two
 21 domains was then calculated. For the RPSC pipes in the urban domain (RPSC-1), it was observed the
 22 effect of building shadow can reduce the thermal performance of the RPSC pipes from 16.82 % to
 23 34.27 %. The obtained minimum PTC values were not less than 8 K or 3.0 % and the maximum
 24 values were not more than 14 K or 5.0 %. Based on the calculated results, the urban RPSC was
 25 36.08% more efficient as compared to the flat/rural RPSC based on the simulation of summer day 21st

1 June at 13:00 hour. The simulation results have shown that the surface within urban canyon absorbed
 2 heat in a diverse range, displaying strong influence of the building geometry on the temperature of the
 3 pavement surface. The calculated STR values of the urban RPSC were between 9.0 % and 14.0 %,
 4 displaying potential of the system to perform 27.11% more in terms of STR when the system was
 5 located within the urban domain.

6
 7 Table 5: Calculated PTC and STR values based on 21st June [36]

Description	$T_{w(i)}$ (K)	$T_{w(o)}$ (K)	Delta T (K)	PTC, %	STR, %
RPSC-0 for all pipes	292.99	301.52	8.53	2.91	9.11
RPSC-1 for all pipes	292.99	304.57	11.58	3.96	11.58
A-5	292.99	306.91	13.92	4.75	13.84
A-4	292.99	306.24	13.25	4.52	13.30
A-3	292.99	305.98	12.99	4.43	13.08
A-2	292.99	305.85	12.86	4.39	12.96
C-1	292.99	305.71	12.72	4.34	12.86
B-2	292.99	303.99	11.00	3.75	11.37
B-3	292.99	302.14	9.15	3.12	9.69
B-4	292.99	302.14	9.15	3.12	9.69
B-5	292.99	302.14	9.15	3.12	9.69
Efficiency (%) of urban RPSC as compared to flat/rural RPSC				36.08	27.11

8

9 **5.2 Analysis based on the changes in system parameters**

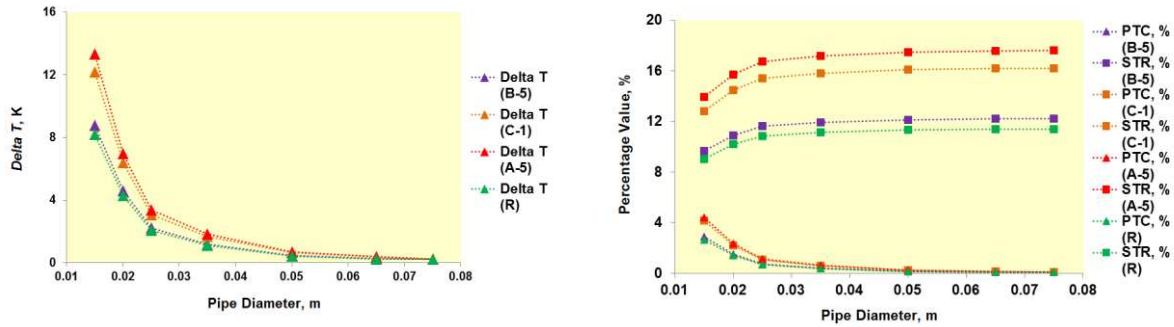
10 Adjustment on the value of four parameters involved with the system was conducted to evaluate the
 11 performance of selected RPSC pipes in urban domain (B-5, C-1 and A-5) and RPSC pipes in flat/rural
 12 domain (B-5, C-1 and A-5 were combined to be R). The result was displayed in the matter of Delta T,
 13 Potential Temperature Collection (PTC, %) and Surface Temperature Reduction (STR, %).

14

15 5.2.1 Effect of changing the diameter of RPSC pipes

16 In this section, the diameter of RPSC pipe was varied between 0.015 m and 0.075 m and the
 17 calculated Delta T, PTC and STR are displayed in Figure 11. Based on Figure 11(a), it was obvious
 18 that the smallest pipe diameter, 0.015 m obtained the highest Delta T which was between 8 K and
 19 13.35 K. Significant reductions were found in the calculated Delta T and the PTC when the diameter
 20 of the RPSC was reduced to 0.020 m; up to 50 % performance drop. In Figure 11(b); the results of
 21 PTC and STR were compared, showing the inverse trend of STR against the trend of PTC. By this; it
 22 can be agreed that the larger the pipe diameter, the higher potential to reduce more surface
 23 temperature. For urban simulation, the highest PTC value was obtained by pipe A-5 with the smallest
 24 pipe diameter while the lowest PTC value was obtained by pipe B-5.

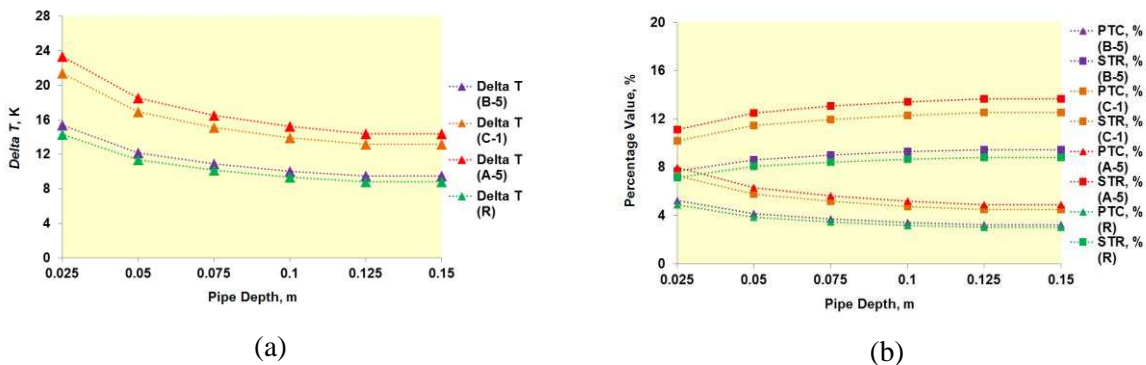
25



1 Figure 11: RPSC performance based on pipe diameter in (a) Delta T (b) PTC and STR

2
3 5.2.2 Effect of changing the depth of RPSC pipes

4 Based on Figure 12, it was observed that the RPSC performance was improved by up 60 % when the
5 pipe depth was reduced from the initial depth of 0.15 m to 0.025 m. A significant drop in the Delta T
6 and the PTC was observed when the depth was increased from 0.025 m to 0.05 m. Simulation of
7 urban domain demonstrated that the highest PTC value was obtained by pipe A-5 at 0.025 m and the
8 lowest PTC value was obtained by pipe B-5 at 0.15 m depth. While, the lowest and the highest STR
9 values obtained were for pipe B-5 and pipe A-5 which were located 0.025 m and 0.15 m below the
10 road surface, respectively.



12 Figure 12: RPSC performance based on pipe depth in (a) Delta T (b) PTC and STR

13
14 5.2.3 Effect of changing the inlet water velocity of RPSC pipes

15 By varying the inlet water velocity of RPSC pipe from 0.1 m/s to 2.0 m/s, the trend of the calculated
16 Delta T, PTC and STR were observed to be similar with the pipe diameter analysis; see Figure 13.
17 The simulation demonstrated a significant reduction in the surface temperature at the early trend
18 (between 0.1 m/s and 0.5 m/s) and slowly dropped influenced by the water temperature which has
19 more dominant on reducing the surface temperature. It can be observed that the Delta T and the PTC
20 will be in an optimum range when the velocity is set not larger than 0.25 m/s. However, it should be
21 noted that huge performance loss when the velocity was changed from the lowest velocity value of 0.1
22 m/s to 0.25 m/s.

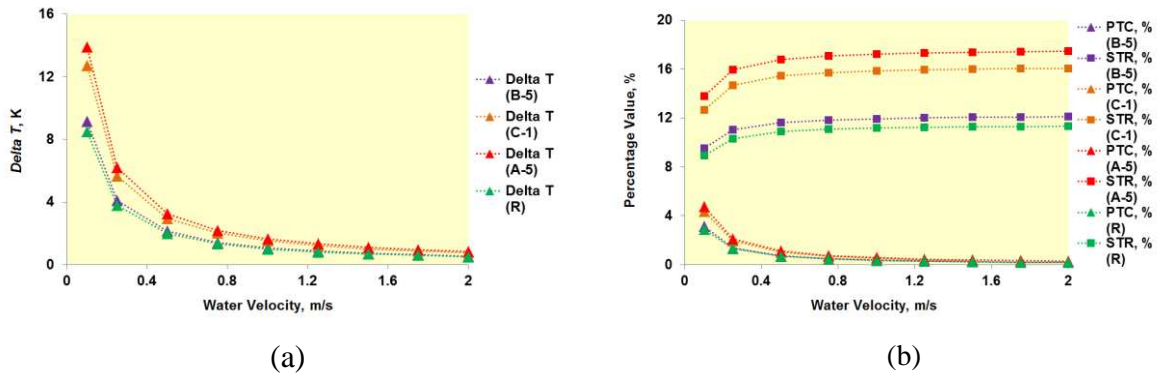


Figure 13: RPSC performance based on water velocity in (a) Delta T (b) PTC and STR

5.2.4 Effect of changing in inlet water temperature

Figure 14 displays the effect of changing the inlet water temperature on the Delta T, PTC and STR values. A constant decrease was observed in the Delta T and PTC when higher temperature was set for the water at the inlet point while a gradual drop was observed in the STR. However, the lowest Delta T can still be obtained above 7.5 K (pipe R, water temperature 298 K) while the highest Delta T can be obtained up to 17 K (pipe A-5, water temperature 278 K).

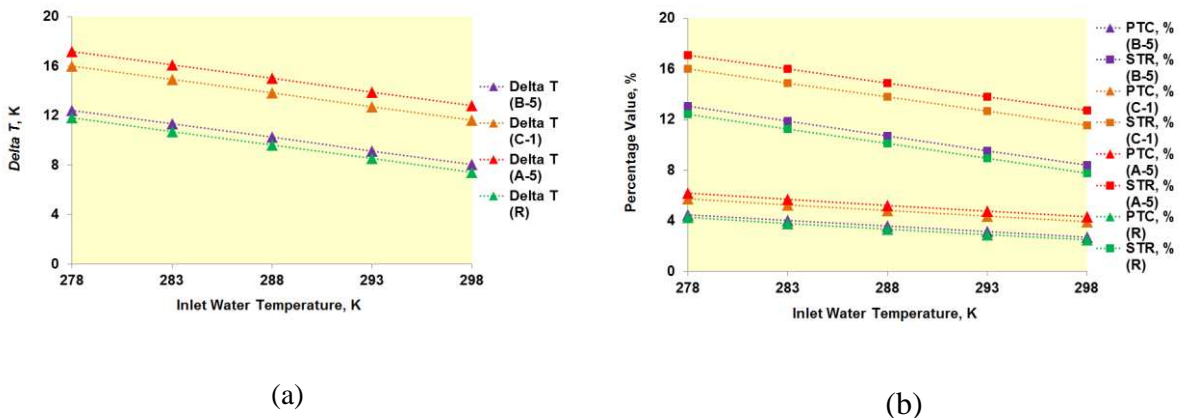


Figure 14: RPSC performance based on inlet water temperature in (a) Delta T (b) PTC and STR

5.3 Comparison in the high-low conditions between urban RPSC and flat/rural RPSC

Table 6 displays the comparison of Delta T, PTC (%) and STR (%) between urban-RPSC and rural-RPSC according to the four parameters, evaluating high and low conditions of the system. The average results of the selected pipes (B-5, C-1 and A-5) were used to represent the urban domain and flat/rural domain. High condition of RPSC performance indicates the maximum value the system can potentially perform and vice-versa for low condition. The analysis demonstrated that the urban RPSC system works the best terms of Delta T and PTC by comparing high and low conditions of pipe depth over the other tested parameters. However, it should be noted that in comparing the application of RPSC in urban domain against flat/rural domain, changing to high condition of pipe diameter, pipe

1 embedment and inlet water velocity shared similar 28.5 % increase in Delta T and PTC followed by
 2 high condition of inlet water temperature, 22.4 %. In comparing between the low conditions of the
 3 tested system parameters, it is worth noting that the inlet water temperature provided the best
 4 percentage difference when comparing the RPSC system application in urban domain against
 5 flat/rural domain; up to 31.5 %.

6
 7 Table 6: Comparative analysis of RPSC performance in two simulated domains

Description	Delta T	PTC (%)	STR (%)
Pipe diameter			
<u>High condition</u>			
▪ Urban domain.....	11.44	3.91	12.13
▪ Flat/rural domain.....	8.18	2.79	9.01
<u>Low condition</u>			
▪ Urban domain.....	0.23	0.08	15.35
▪ Flat/rural domain.....	0.22	0.08	11.41
Pipe depth			
<u>High condition</u>			
▪ Urban domain.....	20.04	6.84	9.66
▪ Flat/rural domain.....	14.32	4.89	7.15
<u>Low condition</u>			
▪ Urban domain.....	11.44	3.91	12.13
▪ Flat/rural domain.....	8.18	2.79	9.01
Inlet water velocity			
<u>High condition</u>			
▪ Urban domain.....	11.92	4.07	12.00
▪ Flat/rural domain.....	8.52	2.91	8.91
<u>Low condition</u>			
▪ Urban domain.....	0.71	0.24	15.21
▪ Flat/rural domain.....	0.51	0.18	11.32
Inlet water temperature			
<u>High condition</u>			
▪ Urban domain.....	15.22	5.47	15.37
▪ Flat/rural domain.....	11.82	4.25	12.44
<u>Low condition</u>			
▪ Urban domain.....	10.82	3.63	10.87
▪ Flat/rural domain.....	7.42	2.49	7.73

8
 9 It was demonstrated that by changing to low condition of pipe diameter, the percentage difference of
 10 Delta T and PTC between the two domains provided the least difference which is 4.6 %. It can be
 11 summarised that the drop in the performance of urban RPSC over flat/rural RPSC was observed up to
 12 84 % when high condition of pipe diameter was changed to the low condition, causing insignificant to
 13 larger the pipe size over 50 % of the diameter. Another insignificant value is less than 0.3 K can be
 14 compared between the urban RPSC and flat/rural RPSC when changing to low condition of both pipe
 15 depth and inlet water velocity. To analyse the comparative study of STR between urban RPSC and
 16 flat/rural RPSC; the highest reduction in the surface temperature was obtained by changing to low

1 condition of inlet water temperature with a value of 28.9 % followed by low condition of pipe
2 diameter and inlet water velocity (25.5 %). Changing from low to high condition of inlet water
3 temperature provides the least difference to compare the urban RPSC and flat/rural RPSC with 19.1
4 %.

5 **6 Discussion**

7 In Section 6.1, the effect of urban canyon on the thermal performance of RPSC system is further
8 discussed. The calculated Delta T, PTC and STR values were analysed and discussed in Section 6.2
9 and the system optimisation was discussed for urban application in Section 6.3.

10 **6.1 Analysis of RPSC embedment inside urban surface and flat surface**

11 Simulation and analysis of the RPSC system during a typical hot summer day demonstrated unequal
12 solar heat flux distribution on the canyon ground surface which was influenced by the building
13 geometry and orientation. Higher surface temperature was observed from the centre of the canyon
14 towards Building A and lower temperature towards Building B. The solar radiation (13:00) has
15 directly heated the surface closer to Building A and was obstructed by Building B which
16 overshadowed about one-third of the road surface. In terms of the air movement, low airflow velocity
17 was observed specifically at the centre of the canyon which caused very low rate of air-solid heat
18 convection at the particular areas. This is a result of the building orientation which caused the wind-
19 blocking effect, causing the wind to cross over and to go through the sides of the buildings with some
20 of the airflow circulating in the canyon space.
21

22
23 Conversely, an evenly distributed temperature was observed for the simulated surface in the rural/flat
24 domain. The simulation of the RPSC on a typical summer day showed that the shadow effect from
25 Building B caused a reduction in the surface temperature between 16.82 % and 34.27 % on average.
26 Furthermore, the RPSC system in the urban domain had a higher average PTC (36.08 %) and higher
27 STR (27.11 %). In the flat/rural domain; it was observed that the overall surface temperature of the
28 canyon ground was lower when the wind flow passed across the surface at a higher speed, causing the
29 heat to be transferred.
30

31 **6.2 Optimisation of Delta T, PTC and STR based on system parameters**

32 **6.2.1 Delta T and PTC**

33 In order to obtain the highest Delta T and PTC; based on the simulation of various design parameters,
34 the RPSC system should be designed with smallest pipe diameter, shallow pipe depth, low water
35 velocity and low inlet water temperature. In this study, the initial pipe depth was 0.15 m below the
36 road surface. At this depth, significant reduction in Delta T and PTC was observed when the pipe
37

1 diameter was increased from 0.015 m to 0.02 m and when the inlet water velocity was increased from
2 0.1 m/s to 0.25 m/s which reduced in the system performance by 50 %. It is worth mentioning that the
3 reduction of 5 K is enough to achieve the standard to prolong the service of the pavement up to 5
4 years [4] and should be the minimum when assessing the RPSC parameters. The shallowest simulated
5 pipe depth provided a Delta T as high as 23 K and as low as 14 K during the hottest time of the
6 simulated summer day. Based on the analysis, the reduction in the pipe depth by 83 % (0.125 m) has
7 increased the Delta T and PTC values by 60 %. Among other tested parameters, the pipe depth
8 parameter had the most potential for energy harvesting while maintaining the optimum pavement
9 lifecycle.

10
11 Of all simulated parameters, adjustment of the inlet water temperature showed the least potential for
12 improving Delta T and PTC and could cost additional energy for reducing/maintaining inlet water
13 temperature. However, it could be useful for adapting to the variation of environmental conditions.
14 Based on the highest simulated inlet water temperature of 298 K, a Delta T of 7.5 K (pipe R) can still
15 be achieved and up to 17 K (pipe A-5) at the lowest simulated inlet water temperature (278 K). Even
16 with the highest simulated temperature, it was clear that the RPSC system still has the potential to
17 increase the lifecycle of the pavement while harvesting thermal energy. Yet, it should be noted that
18 there will be additional cost to keep maintaining the inlet temperature if higher PTC value is required.

19 20 6.2.2 STR value

21 Based on the analysis of pipe diameter and water velocity, it was observed that the STR value was
22 inversely proportional to the decrease in the PTC value. It was observed that there was a sharp
23 increase in the STR value when the pipe diameter was increased from 0.015 m to 0.025 m. Similar
24 trend was observed when the water velocity was increased from 0.1 m/s to 0.5 m/s. By increasing the
25 pipe diameter and the water velocity, more volume of water will be pumped into the pipe which
26 carries lower temperature. This can speed up the heat to be transferred from the road pavement to the
27 RPSC pipe while accelerating the cooling effect in the pavement. However, it was observed that it
28 was unnecessary to increase the pipe diameter and to speed up the water velocity beyond 0.05 m and
29 1.25 m/s. At these diameter and inlet velocity, the temperature of the pavement was found to have
30 reached an equilibrium state with the temperature of the water, demonstrating less and almost no
31 further temperature difference.

32 33 **6.3 System optimisation for urban application**

34 The variation of water velocity in high and low condition to compare the urban and flat domains
35 provided the best performance which was 28 % higher on average higher in terms of PTC and STR
36 over other tested parameters. For urban application, choosing this parameter for optimisation would
37 be ideal due to flexibility in changing the value to meet the requirement and adapt to the

1 environmental conditions without changing the physical properties of the system. Although the
2 highest Delta T can be obtained when reducing the pipe depth, it should be noted that the decision of
3 placing the pipe should be made in the early stage. This is not only to obtain the best PTC and STR
4 but also to consider the best option for protecting the system from long run physical damage
5 especially in heavy traffic condition of urban area. Thus, it is suggested that the design of urban RPSC
6 should consider the inlet water velocity as the main parameter. The embedment depth is optimised for
7 long lifecycle of the pipe and the lifecycle of the pavement in order to obtain a minimum of 5 K
8 reduction.

9 10 **7 Conclusion**

11 Application of the RPSC system was studied by comparing two scenarios, consisting of a simplified
12 urban canyon which represents an urban area and a flat surface which represents a rural area. The ‘de-
13 coupled’ simulation method was employed which couples a macro domain and the micro domain.
14 Based on the simulation and analysis of the RPSC system during a typical hot summer day, it can be
15 summarised that:

- 16 I. The calculated PTC and STR for the RPSC system was 36.08 % and 27.11 % on average higher
17 in the urban domain as compared to the flat/rural domain.
- 18 II. Significant Delta T and PTC values were still obtained in deep pipe embedment and high inlet
19 water temperatures.
- 20 III. A significant drop of 50 in the performance (up to 50 %) was observed when the RPSC pipe
21 diameter and inlet water velocity were increased from 0.015 m to 0.02 m and from 0.1 m/s to
22 0.25 m/s, respectively.
- 23 IV. Low Delta T (lower than 5 K) values were calculated for RPSC system with pipe diameter
24 larger than 0.02 m and with the inlet water velocity higher than 0.25 m/s.
- 25 V. The variation of water velocity in high and low condition to compare the urban domain with
26 flat/rural domain provided the best performance which was 28 % higher on average in terms of
27 both PTC and STR over other tested parameters.

28
29 Based on the results, it can be concluded that buildings and the urban environment have an effect on
30 the best performance of RPSC systems and therefore should be taken into account when carrying out
31 RPSC simulations and parameter optimisation. It should be highlighted that this study evaluates the
32 RPSC performance limited to one building orientation and only during one particular day of
33 summertime. Thus, it should be highlighted that additional studies assessing the influence of external
34 environment on the urban RPSC performance is required to be carried out in the future.

1 **Acknowledgement**

2 This research is supported by Energy 2050 team, The University of Sheffield, United Kingdom.
3 Special gratitude is also given to Malaysia government agency, Majlis Amanah Rakyat (MARA) for
4 the 4 years scholarship of Malaysian postgraduate PhD study.
5

6 **References**

- 7 [1] Tan S., T. Fwa, Influence of Pavement Materials on the Thermal Environment of Outdoor Spaces. *Building and*
8 *Environment*, Vol. 27, No. 3 (1992) pp. 289-295.
- 9 [2] Karunaratne, A., W., Mamparachchi, Modelling of Thermal Effects due to Solar Radiation on Concrete Pavements,
10 University of Moratuwa, Sri Lanka, 2010.
- 11 [3] Hall, M.R., P.K., Dehdezi, A.R., Dawson, J., Grenfell, R., Isola, Influence of the Thermophysical Properties of
12 Pavement Materials on the Evolution of Temperature Depth Profiles in Different Climatic Regions, *Journal of*
13 *Materials in Civil Engineering*, 24 (2012) pp. 32-47.
- 14 [4] Chen, B. L., Bhowmick, S., and Mallick, R. B. (2008). "Harvesting energy from asphalt pavements and reducing the
15 heat island effect." ([http:// users.wpi.edu/~rajib/Draft-2White-Paper-on-Reduce-Harvest-Heat-from-Pavements-Nov-](http://users.wpi.edu/~rajib/Draft-2White-Paper-on-Reduce-Harvest-Heat-from-Pavements-Nov-2008.pdf)
16 [2008.pdf](http://users.wpi.edu/~rajib/Draft-2White-Paper-on-Reduce-Harvest-Heat-from-Pavements-Nov-2008.pdf)) (Jan. 20, 2011).
- 17 [5] Hall, M.R., P.K., Dehdezi, A.R., Dawson, J., Grenfell, R., Isola, Influence of the Thermophysical Properties of
18 Pavement Materials on the Evolution of Temperature Depth Profiles in Different Climatic Regions, *Journal of*
19 *Materials in Civil Engineering*, 24 (2012) pp. 32-47.
- 20 [6] Berdahl, P., S., Bretz, Preliminary Survey of the Solar Reflectance of Cool Roofing Materials, *Energy and Buildings*
21 25 (1997) pp. 149-158.
- 22 [7] Yue, W.S., Z., QiYang, D., YingNa, S., PeiDong, Unidirectional Heat-Transfer Asphalt Pavement for Mitigating the
23 Urban Heat Island Effect, *Journal of Materials in Civil Engineering* 26 (2014) pp. 812-821.
- 24 [8] Akhbari, H., Energy Saving Potentials and Air Quality Benefits of Urban Heat Island Mitigation (2005),
25 <http://www.osti.gov/bridge/servlets/purl/860475-U1H-WIq/860475.PDF>
- 26 [9] Taha, H., Urban Climates and Heat Islands: Albedo, Evapotranspiration, and Anthropogenic Heat, *Energy and*
27 *Buildings* 25 (1997) pp 99-103.
- 28 [10] Erell, E., P. David Boneh, D., Kutiel, P., Bar, Effect of High-Albedo Materials on Pedestrian Heat Stress in Urban
29 Street Canyons, *Urban Climate* (2013).
- 30 [11] Erell, E., Williamson, T., Simulating Air Temperature in an Urban Street Canyon in All Weather Conditions using
31 Measured Data from A Reference Meteorological Station, *Int. J. Climatol.* 26 (2006) pp 1671–1694.
- 32 [12] Pearlmutter, D., Berliner, P., Shaviv, E., Integrated Modeling of Pedestrian Energy Exchange and Thermal Comfort in
33 Urban Street Canyons, *Build. Environ* 42 (2007) pp 2396–2409.
- 34 [13] Vasiliev, L., L., Heat Pipes for Ground Heating and Cooling, *Heat Recovery Systems & CHP* Vol. 8, No. 2 (1987) pp
35 125-138.
- 36 [14] ASHRAE Handbook, HVAC Applications. American Society of Heating, Refrigeration and Air-Conditioning
37 Engineers, Inc., Atlanta, Ga., 1999.
- 38 [15] Bijsterveld W.T., L.J.M., Houben, A., Scarpas, A.A.A., Molenaar, Using Pavement as Solar Collector. Effect on
39 Pavement Temperature and Structural Response, *Transport Research Record* 1778 (17) (2001) pp. 140–148.
- 40 [16] Loomans, M., H., Oversloot, A., D., Bondt, R., Jansen, H., V., Rij, 2003. Design Tool for the Thermal Energy
41 Potential of Asphalt Pavements, Eighth International IBPSA Conference Eindhoven, Netherlands, August (2003) pp
42 11-14.

- 1 [17] Hasebe, M., Y., Kamikawa, S., Meiarashi, Thermoelectric Generators into Solar Thermal Energy in Heated Road
2 Pavement, International Conference on Thermoelectrics, 2006.
- 3 [18] Bobes-Jesus, V., P., Pascual-Muñoz, D., Castro-Fresno, J., Rodriguez-Hernandez, Asphalt Solar Collectors: A
4 Literature Review, Applied Energy 102 (2013) pp. 962–970.
- 5 [19] Wu, S., M. Chen, J., Zhang, Laboratory Investigation into Thermal Response of Asphalt Pavements as Solar Collector
6 by Application of Small-Scale Slabs, Applied Thermal Engineering 31 (2011) pp. 1582-1587.
- 7 [20] Gao, Q., Y., Huang, M., Li, Y., Liu, Y., Y., Yan, Experimental Study of Slab Solar Collection on the Hydronic System
8 of Road, Solar Energy 84 (2010) pp 2096-2102.
- 9 [21] Chen, M., S., Wu, H., Wang, J., Zhang, Study of Ice and Snow Melting Process on Conductive Asphalt Solar
10 Collector, Solar Energy Materials & Solar Cells 95 (2011) pp. 3241–3250.
- 11 [22] Wang, H., S., Wu, M., Chen, Y., Zhang, Numerical Simulation on the Thermal Response of the Heat-Conducting
12 Asphalt Pavement, The Royal Swedish Academy of Sciences Phys. Scr. T139 (2010) pp 014-041.
- 13 [23] Liu, J., S., Wei, M., Changwen, L., Jiaping, Assessment of Fiber Distribution in Steel Fiber Mortar Using Image
14 Analysis, Journal of Wuhan University of Technology-Mater. Sci. Ed. 27 (2012), pp 166-171.
- 15 [24] Chiasson, A., J., D., Spittler, Modeling Approach to Design of a Ground-Source Heat Pump Bridge Deck Heating
16 System. Transport Research Record 1741 Paper No. S00-0054 (2000) pp 207-215.
- 17 [25] Balbay, A., M., Esen, Experimental Investigation of Using Ground Source Heat Pump System for Snow Melting on
18 Pavements and Bridge Decks, Scientific Research and Essays, 5(24) (2010) pp 3955-3966.
- 19 [26] Balbay, A., M., Esen, Temperature Distribution in Pavement and Bridge Slabs Heated by using Vertical Ground-
20 Source Heat Pump Systems, Acta Scientiarum-Technology, 35(4) (2013), pp 677-685.
- 21 [27] Utlu, Z., D., Aydin, O., Kmcay, Comprehensive Thermodynamic Analysis of a Renewable Energy Sourced Hybrid
22 Heating System Combined with Latent Heat Storage, Energy Conversion and Management 84 (2014) pp 311–325.
- 23 [28] Sailor, D.J., H. Fan. Modelling the Diurnal Variability of Effective Albedo for Cities, Atmospheric Environment. 36
24 (2002) pp. 713-725.
- 25 [29] Memon, R.A., D. Y.C. Leung, C. Liu, Effects of Building Aspect Ratio and Wind Speed on Air Temperatures in
26 Urban-Like Street Canyons, Building and Environment 45 (2010) pp. 175-188
- 27 [30] Levermore, G.J., H.K.W., Cheung, S Low Order Canyon Model to Estimate the Influence of Canyon Shape on the
28 Maximum Urban Heat Island Effect, Building Serv. Eng. Res. Technol. 33, 4 (2012) pp. 371-385.
- 29 [31] S. Bottillo, A.D.L., Vollaro, G. Galli, A. Vallati, Fluid Dynamic and Heat Transfer Parameters in an Urban Canyon,
30 Solar Energy 99 (2014) pp. 1-10.
- 31 [32] Allegrini, J., V., Dorer, J., Carmeliet, Coupled CFD, Radiation and Building Energy Model for Studying Heat Flux in
32 An Urban Environment with Generic Building Configurations, Sustainable Cities and Society 19 (2015) pp 385-394.
- 33 [33] E. Bilgen, M.-A. Richard, Horizontal Concrete Slabs As Passive Solar Collector, Solar Energy Vol. 72, No. 5 (2001)
34 pp. 405–413, 2002.
- 35 [34] Georgakis, CH., S., Zoras, M., Santamouris, Studying the Effect of “Cool” Coatings in Street Urban Canyons and its
36 Potential As A Heat Island Mitigation Technique, Sustainable Cities and Society, 13 (2014), pp. 20-31.
- 37 [35] Allegrini, J., V. Dorer, J. Carmeliet, Influence of the Urban Microclimate in Street Canyons on the Energy Demand for
38 Space Cooling and Heating of Buildings, Energy and Buildings 55 (2012) pp. 823-832.
- 39 [36] Nasir D.S.N.M., B., R., Hughes, J., K., Calautit, A Study of the Impact of Building Geometry on the Thermal
40 Performance of Road Pavement Solar Collectors, Energy, 93 (2015) pp 2614-2630.
- 41 [37] Ansys Fluent version 14.0.0, 2011. User’s Guide.
- 42 [38] O’Connor, D., J., K., Calautit, B., R., Hughes, A Study of Passive Ventilation Integrated with Heat Recovery, Energy
43 and Buildings 82 (2014) pp. 799-811.
- 44 [39] Anniballe, R., S., Bonafoni, M., Pichierri, Spatial and Temporal Trends of the Surface and Air Heat Island over Milan
45 using MODIS Data, Remote Sensing of Environment, 150 (2014) pp. 163-171.

- 1 [40] Bulletin of the Polytechnic Institute, Technical University Georghie Asachi, Recommendation for Pipes Selections in
2 Heating and Cooling Systems (2009). Available: <http://www.ce.tuiasi.ro/~bipcons/Archive/62.pdf>
- 3 [41] Wu, S., M., Chen, H., Wang, and Y., Zhang, Laboratory Study on Solar Collector of Thermal Conductive Asphalt
4 Concrete, International Journal of Pavement Research and Technology. 2(4) (2009) pp. 130-136.
- 5 [42] Liou, K-N., Application of the Discrete-Ordinate Method for Radiative Transfer to Inhomogeneous Aerosol
6 Atmospheres, Journal of Geophysical Research, 80 (1975), pp. 3434-3440.
- 7 [43] Uehara, K., S., Murakami, S., Oikawa, S., Wakamatsu, Wind Tunnel Experiments on How Thermal Stratification
8 Affects in and Above Urban Street Canyons, Atmospheric Environment 34 (2000) pp. 1553-1562.
- 9 [44] Elsayed, I., S., M., Mitigation of the Urban Heat Island of the City of Kuala Lumpur, Malaysia, Middle-East Journal of
10 Scientific Research 11 (11) (2012) pp 1602-1613.